Optical dispersion relations in amorphous semiconductors

Sadao Adachi
Department of Electronic Engineering, Faculty of Engineering, Gunma University, Kiryu-shi, Gunma 376, Japan
(Received 17 September 1990; revised manuscript received 13 November 1990)

We report generalized expressions for the optical constants of amorphous (a) semiconductors. The dielectric function spectrum $\epsilon_2(\omega)$ is assumed to yield a continuous absorption obeying the power law $(\hbar\omega)^{-2}(\hbar\omega-E_g)^2$ and have a steep high-energy end at the high-energy cutoff E_c, where E_g is the optical energy gap. The corresponding $\epsilon_1(\omega)$ spectrum shows clear structures both at the E_g and at the E_c edges. By introducing the damping effect into the model, the optical spectra become structureless which are typically observed in amorphous semiconductors. Analyses are presented on the optical dispersion relations of a-Si, a-Ge, and a-GaAs, and the results are in satisfactory agreement with experimental data over the entire range of photon energies (1.5–6.0 eV).

I. INTRODUCTION

Investigation of the dielectric behavior in solids is an old topic which arises in strong connection with the fundamental optical properties of solids. Knowledge of the refractive indices and absorption coefficients of semiconductors is especially important in the design and analysis of various optoelectronic devices. The dielectric function $\epsilon(\omega)=\epsilon_1(\omega)+i\epsilon_2(\omega)$ can describe such an optical response of the medium at all photon energies $E=\hbar\omega$.

Despite the intense interest in amorphous semiconductors for photovoltaic and other device applications, their optical properties are not yet clearly understood especially at high photon energies. Although some measurements (such as reflectivity and spectroscopic ellipsometry) can determine the dielectric-constant dispersion $\epsilon(\omega)$,[1–17] any theoretical calculations of $\epsilon_1(\omega)$ and $\epsilon_2(\omega)$ have not yet been reported.

Pierce and Spicer[18] performed photoemission measurements on amorphous (a-) Si to study the electronic structure and optical properties of the material. They used a conventional retarding-field energy analyzer and a higher-resolution screened-emitter analyzer to measure the energy distribution curves (EDC's) from this material. When the EDC's from crystalline (c-) Si are examined, one finds variations in the position and strength of structure as a result of the conservation of wave vector $\mathbf{k}$ in the crystal. However, in amorphous materials no such variations have been found in the EDC's.[18] This is not unexpected because the absence of long-range order in amorphous materials renders the Bloch theorem inapplicable and leaves the crystalline momentum $\hbar\mathbf{k}$ undefined. They suggested the optical transitions in amorphous semiconductors to be described to a first approximation by the nondirect-transition model in which conservation of energy but not wave vector is significant.[18]

The dielectric constant ϵ_2 for a crystalline semiconductor can be given by

$$\epsilon_2(\omega)=\left[\frac{2\pi e}{m\omega}\right]^2\frac{2}{(2\pi)^3}\times\int_{\mathrm{BZ}}d^3\mathbf{k}|\mathbf{P}_{cv}(\mathbf{k})|^2\delta(E_c(\mathbf{k})-E_v(\mathbf{k})-\hbar\omega)\ , \quad (1)$$

where $\mathbf{P}_{cv}(\mathbf{k})$ is the momentum matrix element $\langle c|p|v\rangle$, c and v denote the conduction and valence bands, respectively, $E_c(\mathbf{k})-E_v(\mathbf{k})$ is the interband energy, and the integration is performed over the first Brillouin zone.

It is well known that the valence and conduction bands retain their meaning even in the amorphous state. Assuming that the basic volume V contains the same number of atoms in the amorphous as in the crystalline states and that $\mathbf{P}_{cv}(\mathbf{k})$ is independent of $\mathbf{k}$, Tauc *et al.*[19,20] obtained

$$\epsilon_2(\omega)=\left[\frac{2\pi e}{m\omega}\right]^2\frac{(2\pi)^3}{2}\frac{1}{B_0}|\mathbf{P}_{cv}|^2\times\int g_c(E^*)g_v(\hbar\omega-E^*)dE^*\ , \quad (2)$$

where g_c and g_v are the densities of states in the conduction and valence bands, respectively. Substituting $g_v(E_p)\sim E_p^{1/2}$, $g_v(E_p)\sim E_p^{1/2}$ into Eq. (2) (where $E_n, E_p, E_n+E_p=\hbar\omega-E_g$ are measured from the band extrema, and E_g is the optical energy gap), they obtained a linear variation of $(\hbar\omega)\epsilon_2^{1/2}$ with $\hbar\omega$:

$$(\hbar\omega)\epsilon_2(\omega)^{1/2}=D^{1/2}(\hbar\omega-E_g)\ , \quad (3)$$

where D is a nondimensional strength parameter and E_g is the optical energy gap.

Weiser and Brodsky[21] also showed that the optical-absorption data in the observable spectral range ($\alpha>10^4$ cm^{-1}) can be remarkably fitted by the expression $\alpha\propto(E-E_g)^2/E$. It is noted that these models are somewhat analogous to the case for the indirect-band-gap transitions in crystalline semiconductors [i.e., $\epsilon_2(E)\propto E^{-2}(E-E_g^{\mathrm{ID}})^2$].[22] Davis and Mott[23] suggested a linear variation of $(En\alpha)^{1/2}$ as the major characteristic of amorphous semiconductors studied experimentally, where n is the refractive index of the medium. More recently, Cody, Brooks, and Abeles[24] reported that a variation of $\epsilon_2^{1/2}$ with E would be an indication of a constant-dipole matrix element for nondirect transitions between simple parabolic bands.

It is evident that it is of both technological importance and scientific interest to have the analytical expressions

of $\epsilon(\omega)$ $[=\epsilon_1(\omega)+i\epsilon_2(\omega)]$ for amorphous materials. The purpose of this paper is to describe the optical properties of amorphous semiconductors in terms of a simplified model of the band structure of the materials. In Sec. II we describe the details of our model, which is an extension of that of Tauc *et al.*[19,20] The $\epsilon_2(\omega)$ spectrum is assumed to yield a continuous absorption obeying the power law $(\hbar\omega)^{-2}(\hbar\omega-E_g)^2$ and have a steep or gradual high-energy end at an appropriately chosen high-energy cutoff E_c. Although the contribution of the nondirect transitions to $\epsilon_2(\omega)$ (or absorption coefficient) is well researched,[19–24] an expression for $\epsilon_1(\omega)$ has not yet been reported to our knowledge. By introducing the high-energy cutoff E_c, we can solve the Kramers-Kronig (KK) relation and obtain the expression for $\epsilon_1(\omega)$. In Sec. III we show the fits with our model to some experimental data (*a*-Si, *a*-Ge, and *a*-GaAs). A satisfactory agreement between our model and experimental data will be achieved over the entire range of photon energies. Finally, in Sec. IV the conclusions obtained in this study are summarized briefly.

II. MODEL

It is noted that the expression (3) is almost identical to that of the indirect optical transitions in crystalline semiconductors:[22,25,26]

$$\epsilon_2(\omega)=\frac{D}{(\hbar\omega)^2}(\hbar\omega-E_g)^2\Theta(1-x_g)\ , \tag{4}$$

with

$$x_g=E_g/\hbar\omega\ , \tag{5}$$

where $\Theta(z)$ is the Heaviside function given by

$$\Theta(z)=\begin{cases}1 & \text{for } z\geq 0\\ 0 & \text{for } z<0\ .\end{cases} \tag{6}$$

The parabolic bands extending to infinite energies implied by Eq. (4) [Eq. (2)] should be nonphysical. We, thus, modify the model by taking into account a high-energy cutoff at the energy E_c. This modification provides[22]

$$\epsilon_2(\omega)=\frac{D}{(\hbar\omega)^2}(\hbar\omega-E_g)^2\Theta(1-x_g)\Theta(1-x_c)\ , \tag{7}$$

with

$$x_c=\hbar\omega/E_c\ . \tag{8}$$

The KK transformation of Eq. (7) gives

$$\epsilon_1(\omega)=1+\frac{2D}{\pi}\left[-\frac{(E_g)^2}{(\hbar\omega)^2}\ln\left|\frac{E_c}{E_g}\right|+\frac{1}{2}\left[1+\frac{E_g}{\hbar\omega}\right]^2\ln\left|\frac{\hbar\omega+E_c}{\hbar\omega+E_g}\right|+\frac{1}{2}\left[1-\frac{E_g}{\hbar\omega}\right]^2\ln\left|\frac{\hbar\omega-E_c}{\hbar\omega-E_g}\right|\right]\ . \tag{9}$$

The $\epsilon_1(\omega)$ spectrum of Eq. (9) exhibits a divergence at E_c. We, therefore, introduce in this expression a damping effect in a phenomenological manner by replacing $\hbar\omega$ by $\hbar\omega+i\Gamma$. The contribution of the optical transitions to $\epsilon(\omega)$ $[\epsilon_1(\omega)=\mathrm{Re}\epsilon(\omega);\ \epsilon_2(\omega)=\mathrm{Im}\epsilon(\omega)]$ in amorphous solids is finally written as

$$\epsilon(\omega)=1+\frac{2D}{\pi}\left[-\frac{E_g^2}{(\hbar\omega+i\Gamma)^2}\ln\left[\frac{E_c}{E_g}\right]+\frac{1}{2}\left[1+\frac{E_g}{\hbar\omega+i\Gamma}\right]^2\ln\left[\frac{\hbar\omega+i\Gamma+E_c}{\hbar\omega+i\Gamma+E_g}\right]+\frac{1}{2}\left[1-\frac{E_g}{\hbar\omega+i\Gamma}\right]^2\ln\left[\frac{\hbar\omega+i\Gamma-E_c}{\hbar\omega+i\Gamma-E_g}\right]\right]\ . \tag{10}$$

The model described above requires four parameters, namely E_g, E_c, D, and Γ. These parameters can be commonly used as adjustable constants for the calculations of both ϵ_2 and ϵ_1. The energy gap E_g and the strength parameter D can be successfully determined from the Tauc plot of $\hbar\omega(\epsilon_2)^{1/2}$ versus $\hbar\omega$ [Eq. (3)]; this plot should give a straight line of slope $D^{1/2}$ and intercept E_g on the energy axis. The parameter values D and E_c must, in principle, be determined from the well-known sum rules

$$\epsilon(0)_{\mathrm{eff}}=1+\frac{2}{\pi}\int_0^{E_m}\frac{\epsilon_2(E)}{E}dE\ , \tag{11a}$$

$$n_{\mathrm{eff}}=\frac{8\pi m\epsilon_0}{Ne^2h^2}\int_0^{E_m}E\epsilon_2(E)dE\ , \tag{11b}$$

where N is the number of atoms per m^3. For *c*-Si ($N=5\times10^{28}$ m^{-3}), $\epsilon(0)_{\mathrm{eff}}=11.7$ and $n_{\mathrm{eff}}=4$ when $E_m\rightarrow\infty$. Note that the microstructure and hence atomic density of amorphous film of any material are strongly dependent on deposition parameters relevant to the preparation technique and process used.[27] It is also known[8] that the optical properties of amorphous materials are strongly influenced by the effects of overlayers (oxide or surface structure) and/or bulk density deficit.

Note that Eq. (10) with $\Gamma=0$ eV diverges at E_c (ϵ_1), but the experimental data do not diverge (see Figs. 2–4). As mentioned in our previous paper, such a divergence can be successfully taken off by introducing the damping effect (see Fig. 2 of Ref. 22). In the limit $\Gamma\rightarrow0$ eV the calculated ϵ_2 spectrum of Eq. (10) exactly agrees with

that of Eq. (7). The damping effect can also smear out the E_g and E_c structural features and, as a result, the optical spectra become structureless which are typically observed in amorphous semiconductors.

III. RESULTS AND DISCUSSION

A. Amorphous Si

We show in Fig. 1 the plots of $(\hbar\omega)\epsilon_2^{1/2}$ versus photon energy $\hbar\omega$ for a-Si [Eq. (3)]. The solid circles are the experimental data taken from Ref. 8 (solid circles). These data were obtained from spectroscopic ellipsometry taken on a low-pressure chemical-vapor-deposited sample on a thermally oxidized c-Si wafer. We can obtain from this figure the optical energy gap $E_g = 1.8$ eV and the strength parameter $D = 117$ for a-Si (solid line).

The fits with our model to the experimental $\epsilon(\omega)$ of a-Si are shown in Fig. 2 (solid lines). The data are taken from Ref. 8 (ϵ_1, solid circles; ϵ_2, open circles). A single broad peak found in the experimental $\epsilon_2(\omega)$ spectrum is typical behavior of amorphous semiconductors. For c-Si, the first-order allowed optical transitions are k-conserved direct transitions, and therefore, the interband spectrum reflects the joint density of states in specific parts of the Brillouin zone [see Eq. (1)].[28,29] The prominent E_1 and E_2 structures in c-Si appear in the spectral region near 3.4 and 4.3 eV, respectively.[29] The disappearance of such structural features in a-Si is due to the breakdown of crystal periodicity in the amorphous material. The experimental data of a-Si give a maximum value of $\epsilon_2 \simeq 30$ near 3.7 eV.[8] The dielectric function exhibiting the largest ϵ_2 at its peak is most representative of a bulk sample of completely coordinated amorphous material. The value of $\epsilon_2 \simeq 30$ has been shown to be an apparently limiting peak value for a-Si, i.e., the corresponding spectrum

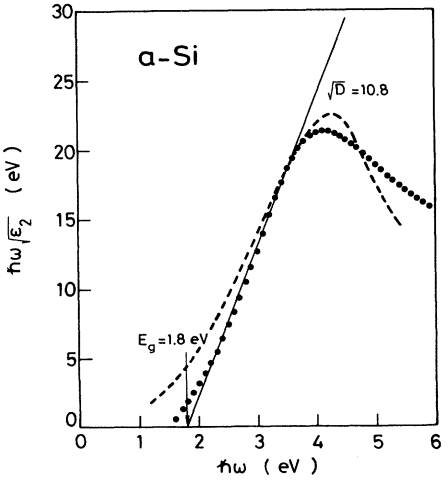

FIG. 1. Plots of $(\hbar\omega)\epsilon_2^{1/2}$ vs $\hbar\omega$ for a-Si. The experimental data are taken from Ref. 8. This plot gives a slope of $D^{1/2} = 10.8$ and intercept $E_g = 1.8$ eV (optical energy gap) on the energy axis (see solid line). The dashed line is also the calculated result taking into account the damping effect ($\Gamma = 0.6$ eV and $D = 172$).

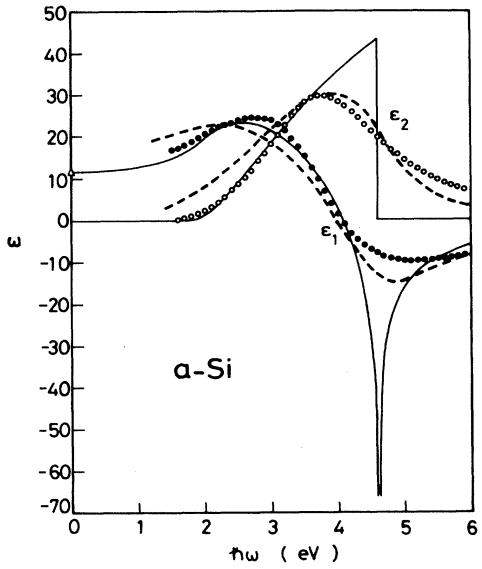

FIG. 2. $\epsilon(\omega)$ spectrum of a-Si (300 K). The experimental data are taken from Ref. 8 (ϵ_1, closed circles; ϵ_2, open circles). The solid lines are obtained from Eq. (10) with the following numerical values: $E_g = 1.8$ eV, $E_c = 4.6$ eV, $D = 117$, and $\Gamma = 0$ eV. The open triangle corresponds to the value of $\epsilon(0)_{\text{eff}}$ ($E_m \to \infty$) [$= 11.7$; see Eq. (11a)] for c-Si. The dashed lines are obtained from Eq. (10) with the following numerical values: $E_g = 1.8$ eV, $E_c = 4.6$ eV, $D = 172$, and $\Gamma = 0.6$ eV.

is thought to be the "intrinsic" dielectric properties of dense a-Si. Similar values have also been obtained by glow discharge,[3] low-pressure chemical-vapor deposition,[4] and multipole plasma-deposition techniques.[7]

The solid lines in Fig. 2 are calculated from Eq. (10) with the following numerical values: $E_g = 1.8$ eV; $E_c = 4.6$ eV; $D = 117$; and $\Gamma = 0$ eV. The cutoff energy E_c ($= 4.6$ eV) has been chosen such that the zero-frequency dielectric constant $\epsilon(0)_{\text{eff}}$ ($E_m \to \infty$) is identical to that for c-Si [$\epsilon(0)_{\text{eff}} = 11.7$]. As evident from Eq. (11a), increasing E_c increases the value of $\epsilon(0)_{\text{eff}}$. The c-Si value of $\epsilon(0)_{\text{eff}}$ is also plotted in the figure by the open triangle. As mentioned in Sec. II, our model with $\Gamma = 0$ eV provides a hard cutoff in the ϵ_2 spectrum at the E_c edge. Also, the model exhibits a divergence in the ϵ_1 spectrum at this energy. Our model, however, successfully explains the experimental $\epsilon(\omega)$ at low photon energies (i.e., below 3.7 eV for ϵ_2 and below 4.1 eV for ϵ_1).

We can remove the disagreeable features at the E_c region by taking account of the damping effect in the model. A comparison of our ϵ model to the experimental data is shown in Fig. 2 by the dashed lines. As discussed in Sec. II, the damping effect can greatly change the spectral features of ϵ. To achieve a better fit, we must therefore use different D values than those used for the solid lines ($\Gamma = 0$ eV). The dashed lines in Fig. 2 are the calculated results with $\Gamma = 0.6$ eV and $D = 172$. The corresponding plot of $(\hbar\omega)\epsilon_2^{1/2}$ versus $\hbar\omega$ is also shown in Fig. 1 by the dashed line.

The damping energy $\Gamma=0.6$ eV derived here seemed to be considerably larger than those of the interband transitions in crystalline materials.[22,25,26,29,30] The damping energy obtained in the crystalline semiconductors can be successfully explained by a sum of two different contributions: $\Gamma(T)=\Gamma_0+\Gamma_\Xi(T)$, where Γ_0 is independent of the temperature T, arising mainly from crystalline imperfections, and $\Gamma_\Xi(T)$ is a contribution through emission and absorption of lattice vibrations (phonons) of average frequency Ξ, proportional to $[\exp(\Xi/T)-1]^{-1}$.[31–33] This expression ensures that the higher the temperature, the larger is the Γ value. Amorphous material preserves the short-range order of the crystal (in this case the tetrahedral coordination), but does not preserve the long-range order. It is, therefore, natural to consider that the large Γ value required in the a-Si analysis is due to the effects of long-range disorder (and short-range defects) in this material. If the main damping mechanism is due to such structural defects, its energy value may not be dependent on the temperature, and therefore, one would predict no significant temperature dependence of the $\epsilon(\omega)$ spectra in amorphous materials.

Introducing the damping effect into the model (dashed lines), we can achieve a reasonable fit with the experiment in the high-energy region (>3.5 eV). On the contrary, however, the fit becomes poorer than that with $\Gamma=0$ eV in the low-energy region. In our model, the strength parameter D is taken to be constant over energies of pair states between the conduction and valence bands. This assumption is usually made in the theory of the optical properties of crystals. If we assume that D is a proper function of energy, the fit will be greatly improved. However, to check the validity of this energy dependence, we will require an exact electronic energy-band structure of the amorphous material, which is still an open question.

B. Amorphous Ge

The fits with our model to the experimental $\epsilon(\omega)$ of a-Ge are shown in Fig. 3. The solid lines are calculated from Eq. (10) with $\Gamma=0$ eV. The data of Connell, Temkin, and Paul[1] on sputtered a-Ge for nearly ideal, void-free material have been quoted (ϵ_1, solid circles; ϵ_2, open circles). This corresponds to a maximum value of $\epsilon_2\simeq 23$, centered at ~ 2.9 eV. Similar results have also been obtained by Theye[2] on evaporated a-Ge.

The plots of $(\hbar\omega)\epsilon_2^{1/2}$ versus $\hbar\omega$ gave the energy gap $E_g=0.85$ eV and the strength parameter $D=50$ for this material. The zero frequency $\epsilon(0)_{\text{eff}}$ for c-Ge is 16 when $E_m\rightarrow\infty$. This value is also plotted in the figure by the open triangle. The cutoff energy of $E_c=4.1$ eV provides the value of $\epsilon_1=16$ ($\hbar\omega=0$ eV), which is the same as the zero-frequency value of c-Ge [i.e., $\epsilon(0)_{\text{eff}}$ ($E_m\rightarrow\infty$)]. The solid lines in Fig. 3 are calculated with these numerical values (i.e., $E_g=0.85$ eV, $E_c=4.1$ eV, $D=50$, and $\Gamma=0$ eV). Like in the case of a-Si, the model gives a good fit with the experimental data at low photon energies (i.e., below 2.6 eV for ϵ_2 and below 3.3 eV for ϵ_1).

The dashed lines in Fig. 3 are the calculated results of our model with $\Gamma\neq 0$ eV. The numerical parameters are the same as those used for the solid lines ($\Gamma=0$ eV), except D (=81) and Γ (=0.9 eV). By considering the damping effect, we can remove the nonphysical, singular features at the E_c region in both the ϵ_2 and ϵ_1 spectra.

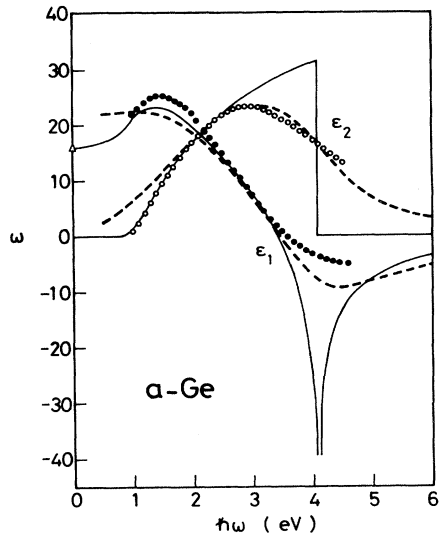

FIG. 3. $\epsilon(\omega)$ spectrum of a-Ge (300 K). The experimental data are taken from Ref. 1 (ϵ_1, solid circles; ϵ_2, open circles). The solid lines are obtained from Eq. (10) with the following numerical values: $E_g=0.85$ eV, $E_c=4.1$ eV, $D=50$, and $\Gamma=0$ eV. The open triangle corresponds to the value of $\epsilon(0)_{\text{eff}}$ ($E_m\rightarrow\infty$) [=16; see Eq. (11a)] for c-Ge. The dashed lines are obtained from Eq. (10) with the following numerical values: $E_g=0.85$ eV, $E_c=4.1$ eV, $D=81$, and $\Gamma=0.9$ eV.

C. Amorphous GaAs

Comparisons of our model to the experimental $\epsilon(\omega)$ spectra for a-GaAs are shown in Fig. 4. The solid and dashed lines are calculated with $\Gamma=0$ and 0.9 eV, respectively. The experimental data are taken from Ref. 9. These data correspond to implantation-amorphized GaAs produced by high-fluency (1×10^{14} cm^{-2}) high-energy (270 keV) As^+ bombardment. It is well known that an energetic ion leaves a trail of defects and dislocations in an otherwise perfect crystal. At sufficiently high-ion fluencies, the damage tracks and the solid become indistinguishable from amorphous material prepared in other ways.[6,9,15–17]

The plots of $(\hbar\omega)\epsilon_2^{1/2}$ versus $\hbar\omega$ gave the optical energy gap $E_g=0.8$ eV and the strength parameter $D=29$ for this material. The $\epsilon(0)_{\text{eff}}$ for c-GaAs is 13.2 when $E_m\rightarrow\infty$. This value is also plotted in Fig. 4 by the open triangle. The cutoff energy of $E_c=5.1$ eV provides the value of $\epsilon_1=13.2$ ($\hbar\omega=0$ eV) which is the same as the zero-frequency value of c-GaAs [i.e., $\epsilon(0)_{\text{eff}}$ ($E_m\rightarrow\infty$)]. The solid lines in Fig. 4 are calculated with these parameters (i.e., $E_g=0.8$ eV, $E_c=5.1$ eV, $D=29$, and $\Gamma=0$ eV). The dashed lines are also obtained with these values, except D (=44) and Γ (=0.9 eV).

As in the case of a-Si and a-Ge, our model with $\Gamma=0$

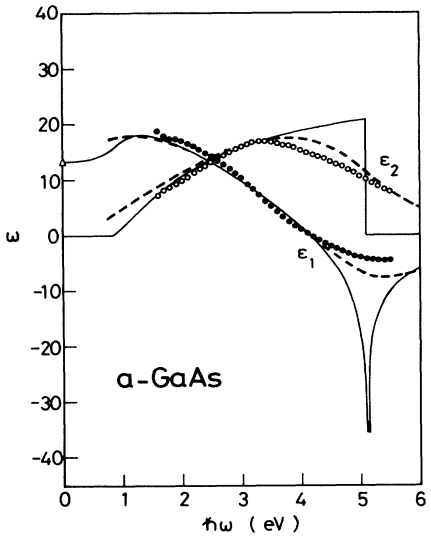

FIG. 4. $\epsilon(\omega)$ spectrum of a-GaAs (300 K). The experimental data are taken from Ref. 9 (ϵ_1, solid circles; ϵ_2, open circles). The solid lines are obtained from Eq. (10) with the following numerical values: $E_g=0.8$ eV, $E_c=5.1$ eV, $D=29$, and $\Gamma=0$ eV. The open triangle corresponds to the value of $\epsilon(0)_{\text{eff}}$ ($E_m\rightarrow\infty$) [$=13.2$; see Eq. (11a)] for c-Ge. The dashed lines are obtained from Eq. (10) with the following numerical values: $E_g=0.8$ eV, $E_c=5.1$ eV, $D=44$, and $\Gamma=0.9$ eV.

eV can explain the spectral dependence of ϵ in the low-energy region (solid lines). The model with $\Gamma=0.9$ eV (and $D=44$) improves the fit at the E_c region, resulting in reasonable agreement with the experiment over the entire range of photon energies (dashed lines).

The cutoff energies (E_c) obtained in the present study are 4.6 eV (a-Si), 4.1 eV (a-Ge), and 5.1 eV (a-GaAs). These energies are found to be nearly the same as the E_2 transition energies in the crystalline substances [$E_2=4.27$ eV (c-Si), 4.35 eV (c-Ge), and 4.7 eV (c-GaAs)]. It is well known that the E_2 peaks dominate in the ϵ_2 spectra of various crystalline substances. The ϵ_2 spectra of As^+-implanted GaAs showed[9] that one of the main features induced by ion implantation is a gradual smearing out of the E_1 and E_2 structures by damage clusters. The peak value of ϵ_2, which is related to the intensity of interband absorption, drastically falls with increasing damage. The E_2 peak finally disappears for high doses. We were, however, not able to explain why the E_c energy has nearly the same value as the E_2 energy gap.

IV. CONCLUSIONS

We have presented a method for the calculations of the real (ϵ_1) and imaginary (ϵ_2) parts of the dielectric function of amorphous semiconductors. The model is based on the Kramers-Kronig transformation and assumes that the $\epsilon_2(\omega)$ spectrum yields a continuous absorption obeying the power law $(\hbar\omega)^{-2}(\hbar\omega-E_g)^2$ and a steep high-energy end at the cutoff energy E_c. The transition strength parameter is also taken to be constant over energies of pair states between the conduction and valence bands. The corresponding $\epsilon_1(\omega)$ spectrum shows a weak structure at the optical energy gap E_g and a strong negative peak at the E_c edge. Introducing the damping effect into the model, the calculated spectra resemble those typically observed in amorphous materials. Detailed analyses are presented for a-Si, a-Ge, and a-GaAs, and the results obtained are in reasonable agreement with the experimental data over the entire range of photon energies (1.5–6.0 eV). If one assumes that the strength parameter is a proper function of energy, the fit can be further improved. Dielectric-related optical constants, such as the refractive indices and the absorption coefficients, are easy to obtain from the present study in analytical functional forms.

ACKNOWLEDGMENT

This work was supported in part by the Gunma University Foundation for Science and Technology, Gunma, Japan.

[1]G. A. N. Connell, R. J. Temkin, and W. Paul, Adv. Phys. **22**, 643 (1973).

[2]M. L. Theye, in *Amorphous and Liquid Semiconductors*, edited by J. Stuke and W. Brenig (Taylor and Francis, London, 1974), p. 479.

[3]D. Ewald, M. Milleville, and G. Weiser, Philos. Mag. B **40**, 291 (1979).

[4]B. G. Bagley, D. E. Aspnes, A. C. Adams, and F. B. Alexander, Jr., Bull. Am. Phys. Soc. **25**, 12 (1980).

[5]B. G. Bagley, D. E. Aspnes, A. C. Adams, and C. J. Mogab, Appl. Phys. Lett. **38**, 56 (1981).

[6]D. E. Aspnes, S. M. Kelso, C. G. Olson, and D. W. Lynch, Phys. Rev. Lett. **26**, 1863 (1982).

[7]B. Drevillon, J. Perrin, J. M. Siefert, J. Huc, A. Lloret, G. de Rosny, and J. P. M. Schmitt, Appl. Phys. Lett. **42**, 801 (1983).

[8]D. E. Aspnes, A. A. Studna, and E. Kinsbron, Phys. Rev. B **29**, 768 (1984).

[9]M. Erman, J. B. Theeten, P. Chambon, S. M. Kelso, and D. E. Aspnes, J. Appl. Phys. **56**, 2664 (1984).

[10]R. W. Collins, A. H. Clark, S. Guha, and C.-Y. Huang, J. Appl. Phys. **57**, 4566 (1985).

[11]K. Mui, D. K. Basa, F. W. Smith, and R. Corderman, Phys. Rev. B **35**, 8089 (1987).

[12]B. Drevillon and C. Godet, J. Appl. Phys. **64**, 145 (1988).

[13]T. V. Herak, J. J. Schellenberg, P. K. Shufflebotham, and K. C. Kao, J. Appl. Phys. **64**, 688 (1988).

[14]G. B. Smith and D. R. McKenzie, J. Appl. Phys. **65**, 1694 (1989).

[15]G. F. Feng and R. Zallen, Phys. Rev. B **40**, 1064 (1989).

[16]X.-F. He, R.-R. Jiang, R.-X. Chen, and D. Mo, J. Appl. Phys.

66, 5261 (1989).
[17]A. Borghesi, A. Piaggi, A. Stella, G. Guizzetti, D. Bisero, and G. Queirolo, J. Appl. Phys. **67**, 7045 (1990).
[18]D. T. Pierce and W. E. Spicer, Phys. Rev. B **5**, 3017 (1972).
[19]J. Tauc, R. Grigorovici, and A. Vancu, Phys. Status Solidi **15**, 627 (1966).
[20]J. Tauc, in *Optical Properties of Solids,* edited by F. Abeles (North-Holland, Amsterdam, 1972), p. 277.
[21]K. Weiser and M. H. Brodsky, Phys. Rev. B **1**, 791 (1970).
[22]S. Adachi, Phys. Rev. B **41**, 3504 (1990).
[23]E. A. Davis and N. F. Mott, Philos. Mag. **22**, 903 (1970).
[24]G. D. Cody, B. G. Brooks, and B. Abeles, Solar Energy Mat. **8**, 231 (1982).
[25]S. Adachi, J. Appl. Phys. **67**, 6427 (1990).
[26]S. Adachi, J. Appl. Phys. **68**, 1192 (1990).
[27]K. L. Chopra, *Thin Film Phenomena* (McGraw-Hill, New York, 1969).
[28]D. E. Aspnes and A. A. Studna, Phys. Rev. B **27**, 985 (1983).
[29]S. Adachi, Phys. Rev. B **38**, 12 966 (1988).
[30]S. Adachi, Phys. Rev. B **41**, 1003 (1990).
[31]P. Lautenschlager, M. Garriga, L. Viña, and M. Cardona, Phys. Rev. B **36**, 4821 (1987).
[32]L. Viña, S. Logothetidis, and M. Cardona, Phys. Rev. B **30**, 1979 (1984).
[33]P. Lautenschlager, M. Garriga, S. Logothetidis, and M. Cardona, Phys. Rev. B **35**, 9174 (1987).